J Therm Anal Calorim (2012) 108:895–900
DOI 10.1007/s10973-012-2356-9

Crystal growth, structure and characterization of *o*-hydroxybenzoic acid single crystals

Solvent effects

V. Meenatchi · K. Muthu · M. Rajasekar · S. P. Meenakshisundaram · S. C. Mojumdar

CTAS2011 Conference Special Chapter

Abstract Single crystals of *o*-hydroxybenzoic acid (*o*-HBA, salicylic acid) have been grown by slow evaporation solution growth technique. It crystallizes in monoclinic system with two molecular units in the cell (centrosymmetric space group $P2_1/c$). The lattice parameters are $a = 4.8967(6)$ Å, $b = 11.2204(14)$ Å, $c = 11.3027(15)$ Å and $\beta = 92.096(12)°$. The modes of vibrations of different functional groups present were identified by FT-IR studies. Differential scanning calorimetry (DSC) study reveals the purity of the sample and no decomposition is observed up to the melting point. The crystals are further characterized using UV–Vis and powder XRD. Effect of solvents on the growth and morphology has been investigated. The crystalline cohesion is achieved by intra and intermolecular hydrogen bonds.

Keywords Crystal growth · DSC · FT-IR spectra · XRD analysis · Carboxylic acid · SEM analysis

Introduction

o-Hydroxybenzoic acid (*o*-HBA) and its derivatives are one of the organic biomolecules subjected to intensive research as it represents a great interest for a wide range of applications in medicines, agriculture, photosynthesis etc. [1–5]. Salicylic acid micrometre scale (2–5 μm length) crystallization in ethanol/methanol as solvent by slow evaporation solution growth technique at low temperature (278 K) has been reported [6]. By solventless thermal crystallization method needle-like salicylic acid crystals of 10–12 mm in length have been grown [7]. Guo et al. [8] and Zhang et al. [9] have prepared needle-like salicylic acid crystallites with average diameters of 34 and 16 μm, respectively, by neutralizing sodium salicylate with hydrochloric acid. Domingo et al. [10] have synthesized needle-like salicylic acid crystallites of 2–5 μm length with 2 μm diameter by supercritical technology. Salicylic acid has a significantly lower solubility in water compared to organic solvents [11]. It crystallizes as hallow tubes with square cross-sectional areas from water. The cell parameters have been determined, and structure is in close agreement with the reported values [6, 12–14]. Thermal and spectral analyses are very useful methods for materials' characterization. Therefore, many authors have used these techniques for various materials' characterization [15–35]. In this paper, we are reporting the bulk growth of salicylic acid crystals in different solvents and mixed solvent systems. The as-grown crystal in water–methanol (1:2 v/v) is subjected to characterization studies.

V. Meenatchi · K. Muthu · M. Rajasekar · S. P. Meenakshisundaram
Department of Chemistry, Annamalai University, Annamalainagar 608 002, Tamilnadu, India

S. C. Mojumdar (✉)
Department of Chemistry, University of Guelph, Guelph, ON, Canada
e-mail: scmojumdar@yahoo.com

S. C. Mojumdar
Department of Chemical Technologies and Environment, Faculty of Industrial Technologies, Trenčín University of A. Dubček, 020 32 Púchov, Slovakia

Experimental

Crystal growth

Single crystals of *o*-HBA were grown by slow evaporation solution growth technique. A saturated solution of *o*-HBA was prepared in different solvents. The solution was stirred

well and left for slow evaporation at room temperature. Numerous tiny crystals were formed at the bottom of the container due to spontaneous nucleation within 3–5 days. Good optical quality crystals were harvested after a period of 7–8 days. The photographs of as-grown crystals of *o*-HBA are shown in Fig. 1.

Measurements

The FT-IR spectra were recorded using an AVATAR 330 FT-IR instrument by the KBr pellet technique in the range 500–4,000 cm^{-1}. The single-crystal structure of *o*-HBA was carried out from a selected colourless tablet of approximately $0.33 \times 0.28 \times 0.23$ mm^3. Crystal data were collected and integrated using an Oxford Diffraction Xcalibur-S CCD system equipped with graphite monochromated MoK_α ($\lambda = 0.71073$ Å) radiation. The powder X-ray diffractometer (XRD) analysis was performed on a Philips Xpert Pro Triple-axis X-ray diffractometer. The XRD data are analysed by Rietveld method with RIETAN-2000. The UV–vis analysis of *o*-HBA crystal was carried out between 200 and 800 nm, using the Perkin Elmer Lambda 35 model spectrophotometer. Differential scanning calorimetric (DSC) study was performed on a NETZSCH DSC 204 in the temperature range 0–300 °C at a heating rate of 50 °C/min in the nitrogen atmosphere. The surface morphology was observed on a JEOL JSM 5610 LV scanning electron microscope.

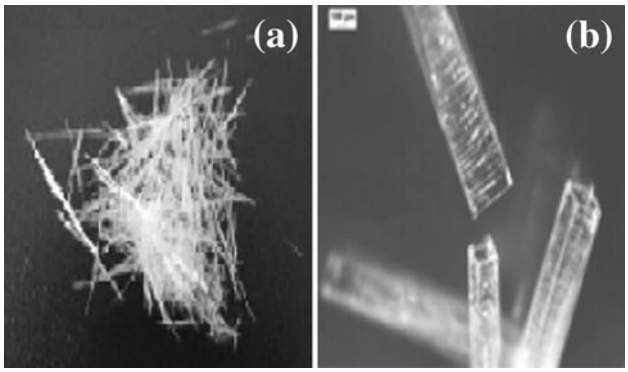

Fig. 2 Photographs of *o*-HBA crystals already reported **a** solventless thermal crystallization method [7] **b** in water (×32) [11]

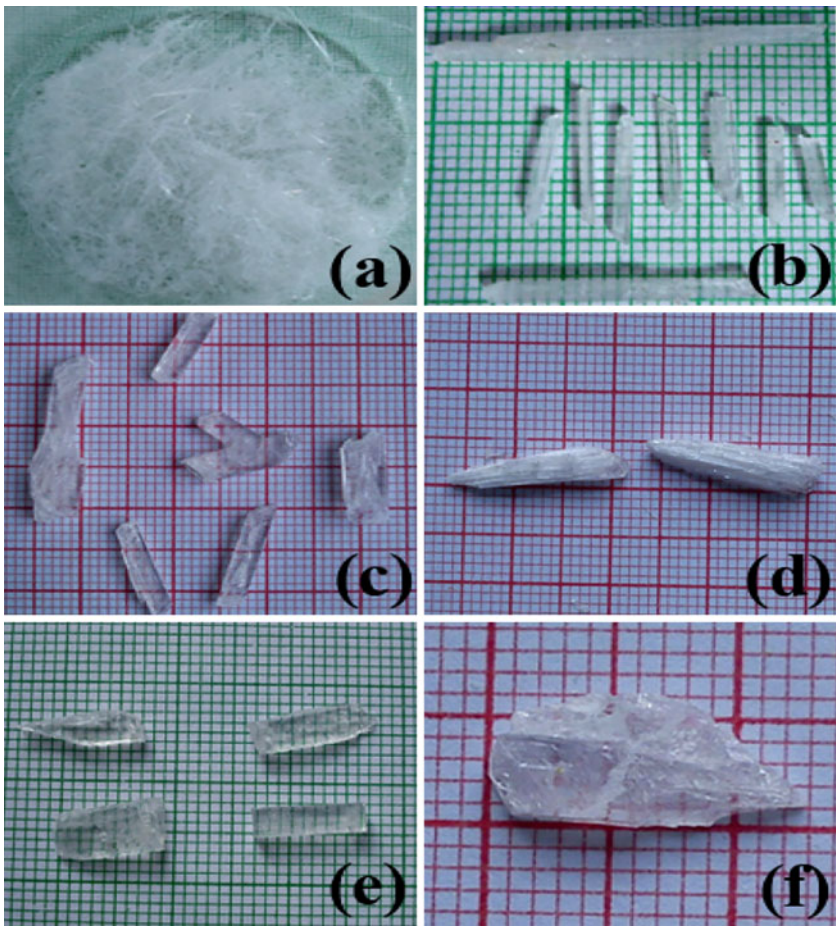

Fig. 1 Photographs of as-grown *o*-HBA crystals in various solvents: **a** methanol, **b** water–methanol. **c** ethanol, **d** water–ethanol, **e** acetonitrile, **f** water–acetonitrile

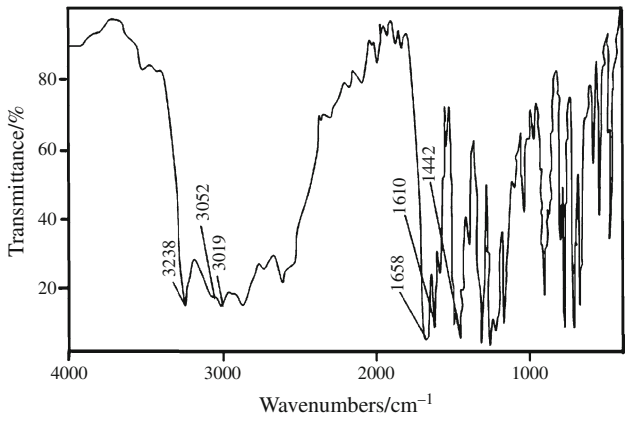

Fig. 3 FT-IR spectrum of *o*-HBA crystal

Table 1 Fundamental vibrations of *o*-HBA (wavenumber/cm^{-1})

o-HBA	Assignment of vibration
3,238	ν_{-OH}
3,052 and 3,019	ν_{CH}
1,658	$\nu_{C=O}$
1,610 and 1,442	$\nu_{C=C}$

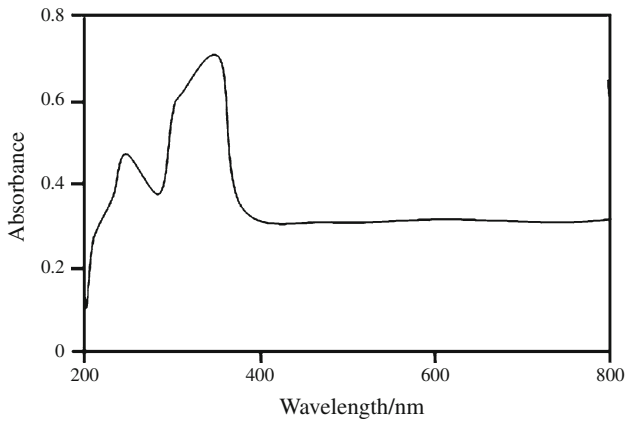

Fig. 4 UV–Vis spectrum of *o*-HBA crystal

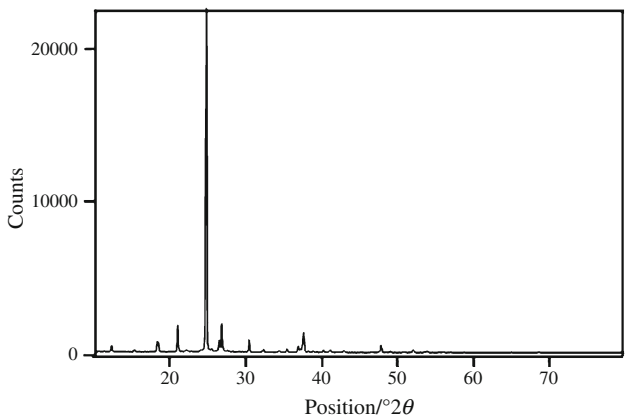

Fig. 5 Powder X-ray diffraction curve of *o*-HBA

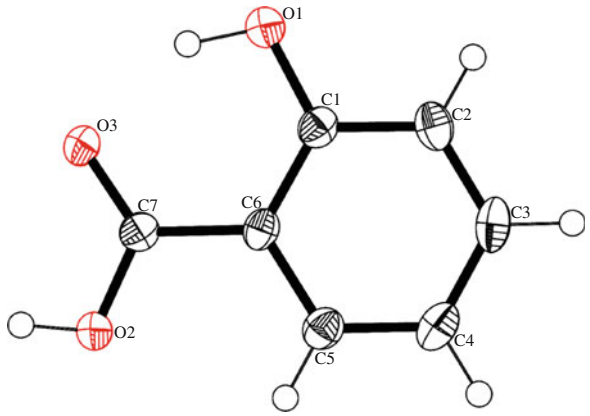

Fig. 6 ORTEP diagram of *o*-HBA crystal

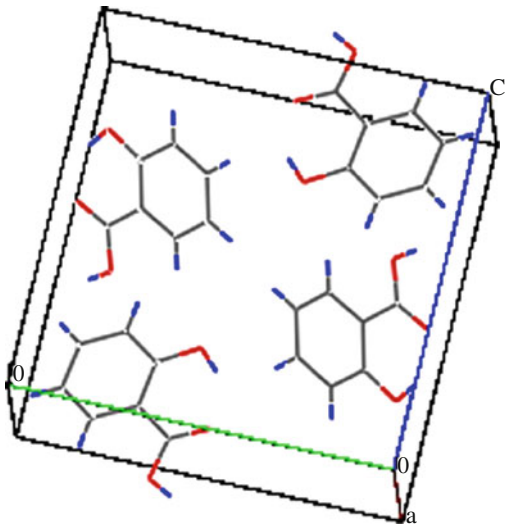

Fig. 7 Packing diagram of *o*-HBA crystal

Table 2 Crystal data of *o*–hydroxybenzoic acid single crystals

	o–HBA	Reported[a]
Molecular formula	$C_7H_6O_3$	$C_7H_6O_3$
Molecular weight	138.12/g/mol	138.10/g/mol
Unit cell parameters	$a = 4.8967(6)/\AA$	$a = 4.926(2)/\AA$
	$b = 11.2204(14)/\AA$	$b = 11.230(5)/\AA$
	$c = 11.3027(15)/\AA$	$c = 11.565(6)/\AA$
	$\beta = 92.096(12)/°$	$\beta = 90.77(4)/°$
Crystal size	0.33 × 0.28 × 0.23/mm^3	0.12 × 0.20 × 0.80/mm^3
Volume	$620.59(14)/\AA^3$	$639.8(6)/\AA^3$
Colour	Colourless	Colourless
Crystal system	Monoclinic	Monoclinic
Space group	$P2_1/c$	$P2_1/c$
Z	2	4
Calculated density	1.478/g/cm^3	1.434/g/cm^3
Radiation (λ, Å)	Mo-Kα (0.71073)	Mo-Kα (0.71073)
Temperature	150 (2)/K	293/K

[a] Ref [7]

Table 3 Hydrogen bond geometry/Å, °

D–H···A	D–H	H···A	D···A	D–H···A
O1–H(101)···O3	0.96(3)	1.77(3)	2.6210(18)	146(3)
O2–H(102)···O3	0.91(2)	1.75(2)	2.6574(18)	174(2)
C2–H2···O2	0.95	2.58	3.320(2)	135

Symmetry codes: (i) $-x, -y, 1-z$; (ii) $1+x, 1/2-y, -1/2+z$

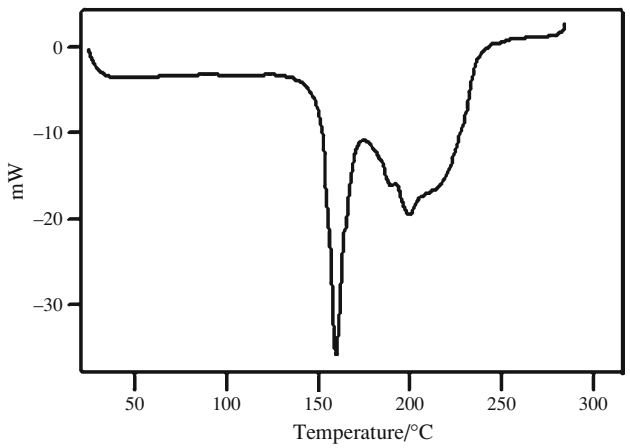

Fig. 8 DSC curve of *o*-HBA crystal

Results and discussion

The photographs of salicylic acid crystals grown by different techniques by various investigators are displayed in Fig. 2. It appears from the crystal photos that the quality and size of the crystal depends on the nature of the solvent.

The various functional groups of *o*-HBA are confirmed by recording the FT-IR spectrum in the range 4,000–500 cm^{-1} (Fig. 3) and the assignments of well-defined bands are given in Table 1. In the FT-IR spectrum, the broad band at 3,238 cm^{-1} is unambiguously attributed to the phenolic –OH stretch, which is intramolecular hydrogen bonded to the carbonyl oxygen [36]. The bands around 3,100–3,000 cm^{-1} are assigned to –CH stretching frequency. The presence of intramolecular hydrogen bonding between the hydroxyl hydrogen atom and the carboxyl oxygen atom reduces the –C=O stretching frequency (1,685 cm^{-1}). The UV spectrum (Fig. 4) reveals that the cut off λ is $\backsim$350 nm. Absorption is minimum in the 390–800 nm range. A good transparency in the visible region is a great advantage for optical applications.

The powder XRD patterns of *o*-HBA crystals (Fig. 5) show that the sample is of single phase without detectable impurity. Narrow peaks indicate the good crystallinity of the material. The structural properties of the grown crystals depend on the state of the synthesized and the orientations of the as-grown crystals. The structure of *o*-HBA single crystal is confirmed by single crystal XRD analysis and it is very well shown in the ORTEP and packing diagrams (Figs. 6, 7). It crystallizes in the monoclinic crystal system with a space group of $P2_1/c$ and crystal data are given in the Table 2. These values are in good agreement with the reported values [7]. The usual intramolecular hydrogen bond is found between the phenolic hydrogen atom and carboxylate oxygen atom of (O1-H(101)–O3) *o*-HBA

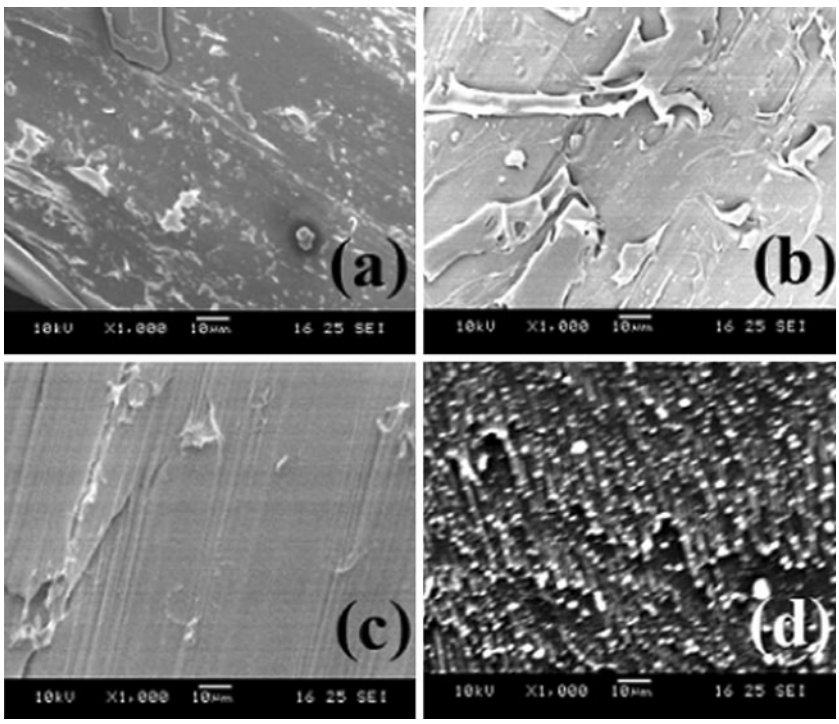

Fig. 9 SEM images of *o*-HBA crystal **a** methanol **b** water–methanol **c** ethanol **d** acetonitrile

molecule, where the proton is located on the phenol group rather than the carboxyl group [37]. Hydrogen bonding interactions of *o*-HBA molecule are listed in Table 3.

The DSC was performed to know the thermal behaviours of the grown crystals. This analysis clearly shows that there is no physically adsorbed water in the molecular structure of crystals. The studies reveal the purity of the material. DSC (Fig. 8) shows that the melting point of crystal is ∽159 °C. The compound is stable and there is no phase transition till it is melting. No decomposition up to the melting point ensures the suitability of the material for application in lasers where the crystals are required to withstand high temperatures. The sharp endothermic peak indicates the solid state transition for relatively pure material. The melting point of *o*-HBA molecule was also determined by using Sigma instrument melting point apparatus (155 °C).

The effect of solvents on the surface morphology of *o*-HBA crystals are shown in Fig. 9. Varied morphologies in different solvent systems could be due to solute–solvent affinity. In methanol as solvent scatter centres are visible. The crystallites were composed of bar-like and spherical particles in water–ethanol (1:2 v/v) medium. A plate-like morphology with scattered centers results in ethanol. Uniform diameter pores are revealed in the SEM picture of acetonitrile grown crystals.

Conclusions

The *o*-hydroxybenzoic acid single crystals in different solvents and mixed solvent systems have been successfully grown by conventional (SEST) solution growth method. The various vibrational modes present in the *o*-HBA molecule are well explained by FT-IR spectroscopy. The crystallographic data indicate that the *o*-HBA molecules are crystallizing in monoclinic system with centrosymmetric space group $P2_1/c$. The UV–visible spectrum of *o*-HBA showed that the crystal is transparent in the range ∽380–800 nm. Thermal behaviour has been assessed by DSC analysis. This study reveals that the compound is stable up to its melting point (∽159 °C). SEM studies reveal the external morphological changes with solvent systems.

References

1. Yao H, Tian S. Effects of pre- and post-harvest application of salicylic acid or methyl jasmonate on inducing disease resistance of sweet cherry fruit in storage. Postharvest Biol Technol. 2005;35:253–62.
2. Cleland CF, Ajami A. Identification of the flower-inducing factor isolated from aphid honeydew as being salicylic acid. Plant Physiol. 1974;54:904–6.
3. Noreen S, Ashraf M. Alleviation of adverse effects of salt stress on sunflower (*Helianthus annuus* l.) by exogenous application of salicylic acid: growth and photosynthesis. Pak J Bot. 2008;40:1657–63.
4. Khan W, Prithiviraj B, Smith DL. Photosynthetic responses of corn and soybean to foliar application of salicylates. J Plant Physiol. 2003;160:485–92.
5. Nakamura J, Inoue Y, Sasaki H, Shibasaki J. Prolonged blood concentration of salicylic acid following the simultaneous oral administration of salicylic acid and salicyluric acid in rabbits. Chem Pharm Bull (Tokyo). 1986;34:2624–7.
6. Munshi P, Guru Row TN. Intra- and intermolecular interaction in small bio active molecules; cooperative features from experimental and theoretical charge-density analysis. Acta Crystallogr B. 2006;62:612–26.
7. Menaa B, Takahashi M, Tokuda Y, Yoko T. Characterization and solventless growth of salicylic acid macro-crystals involving a nitrogen gas flow. Cryst Res Technol. 2010;45:341–6.
8. Guo G, Cai Y, Mei J. J Pharm Chin. 1999;15:44.
9. Zhang W, Dai J, Zhang Y, Pu ZJ. China Pharm Univ. 1997;28:215.
10. Domingo C, Berends E, Rosmalen GM. Precipitation of ultrafine organic crystals from the rapid expansion of supercritical solutions over a capillary and a frit nozzle. J Supercrit Fluids. 1997;10:39–55.
11. Nordstrom FL, Rasmuson AC. Solubility and melting properties of salicylic acid. J Chem Eng Data. 2006;51:1668–71.
12. Cochran W. The crystal structure of salicylic acid. Acta Crystallogr. 1951;4:376–7.
13. Cochran W. The crystal and molecular structure of salicylic acid. Acta Crystallogr. 1953;6:260–8.
14. Sundaralingham M, Jensen LH. Refinement of the structure of salicylic acid. Acta Crystallogr. 1965;18:1053–8.
15. Mojumdar SC, Raki L. Preparation, thermal, spectral and microscopic studies of calcium silicate hydrate-poly(acrylic acid) nanocomposite materials. J Therm Anal Calorim. 2006;85:99–105.
16. Sawant SY, Verenkar VMS, Mojumdar SC. Preparation, thermal, XRD, chemical and FT-IR spectral analysis of $NiMn_2O_4$ nanoparticles and respective precursor. J Therm Anal Calorim. 2007;90:669–72.
17. Porob RA, Khan SZ, Mojumdar SC, Verenkar VMS. Synthesis, TG, SDC and infrared spectral study of $NiMn_2(C_4H_4O_4)_3{\cdot}6N_2H_4$—a precursor for $NiMn_2O_4$ nanoparticles. J Therm Anal Calorim. 2006;86:605–8.
18. Mojumdar SC, Varshney KG, Agrawal A. Hybrid fibrous ion exchange materials: past, present and future. Res J Chem Environ. 2006;10:89–103.
19. Doval M, Palou M, Mojumdar SC. Hydration behaviour of C_2S and C_2AS nanomaterials, synthesized by sol–gel method. J Therm Anal Calorim. 2006;86:595–9.
20. Mojumdar SC, Moresoli C, Simon LC, Legge RL. Edible wheat gluten (WG) protein films: preparation, thermal, mechanical and spectral properties. J Therm Anal Calorim. 2011;104:929–36.
21. Varshney G, Agrawal A, Mojumdar SC. Pyridine based cerium(IV) phosphate hybrid fibrous ion exchanger: synthesis, characterization and thermal behaviour. J Therm Anal Calorim. 2007;90:731–4.
22. Mojumdar SC, Melnik M, Jona E. Thermal and spectral properties of Mg(II) and Cu(II) complexes with heterocyclic N-donor ligands. J Anal Appl Pyrolysis. 2000;53:149–60.
23. Borah B, Wood JL. Complex hydrogen bonded cations. The benzimidazole benzimidazolium cation. Can J Chem. 1976;50:2470–81.
24. Mojumdar SC, Sain M, Prasad RC, Sun L, Venart JES. Selected thermoanalytical methods and their applications from medicine to construction. J Therm Anal Calorim. 2007;60:653–62.

25. Meenakshisundarm SP, Parthiban S, Madhurambal G, Mojumdar SC. Effect of chelating agent (1,10-phenanthroline) on potassium hydrogen phthalate crystals. J Therm Anal Calorim. 2008;94:21–5.
26. Rejitha KS, Mathew S. Investigations on the thermal behavior of hexaamminenickel(II) sulphate using TG-MS and TR-XRD. Glob J Anal Chem. 2010;1(1):100–8.
27. Pajtášová M, Ondrušová D, Jóna E, Mojumdar SC, Ľalíková S, Bazyláková T, Gregor M. Spectral and thermal characteristics of copper(II) carboxylates with fatty acid chains and their benzothiazole adducts. J Therm Anal Calorim. 2010;100:769–77.
28. Madhurambal G, Ramasamy P, Anbusrinivasan P, Vasudevan G, Kavitha S, Mojumdar SC. Growth and characterization studies of 2-bromo-4′-chloro-acetophenone (BCAP) crystals. J Therm Anal Calorim. 2008;94:59–62.
29. Gonsalves LR, Mojumdar SC, Verenkar VMS. Synthesis and characterisation of $Co_{0.8}Zn_{0.2}Fe_2O_4$ nanoparticles. J Therm Anal Calorim. 2011;104:869–73.
30. Raileanu M, Todan L, Crisan M, Braileanu A, Rusu A, Bradu C, Carpov A, Zaharescu M. Sol–gel materials with pesticide delivery properties. J Environ Prot. 2010;1:302–13.
31. Varshney KG, Agrawal A, Mojumdar SC. Pectin based cerium(IV) and thorium(IV) phosphates as novel hybrid fibrous ion exchangers synthesis, characterization and thermal behaviour. J Therm Anal Calorim. 2005;81:183–9.
32. Mojumdar SC, Šimon P, Krutošíková A. [1]Benzofuro[3,2-c]pyridine: synthesis and coordination reactions. J Therm Anal Calorim. 2009;96:103–9.
33. Moricová K, Jóna E, Plško A, Mojumdar SC. Thermal stability of Li_2O–SiO_2–TiO_2 gels evaluated by the induction period of crystallization. J Therm Anal Calorim. 2010;100:817–20.
34. Mojumdar SC, Miklovic J, Krutosikova A, Valigura D, Stewart JM. Furopyridines and furopyridine-Ni(II) complexes—Synthesis, thermal and spectral characterization. J Therm Anal Calorim. 2005;81:211–5.
35. Vasudevan G, AnbuSrinivasan P, Madhurambal G, Mojumdar SC. Thermal analysis, effect of dopants, spectral characterisation and growth aspects of KAP crystals. J Therm Anal Calorim. 2009;96:99–102.
36. El Nasr E, Fujii A, Yahagi T, Ebata T, Mikami N. Laser spectroscopic investigation of salicylic acids hydrogen bonded with water in supersonic jets: microsolvation effects for excited state proton dislocation. J Phys Chem A. 2005;109:2498–504.
37. Smith G, Wermuth UD, White JM. Acta Crystallogr E. 2002;58:o1315–7.